

# Spin noise spectroscopy to probe quantum states of ultracold fermionic atomic gases

Bogdan Mihaila,<sup>1</sup> Scott A. Crooker,<sup>2</sup> Krastan B. Blagoev,<sup>1</sup>  
Dwight G. Rickel,<sup>2</sup> Peter B. Littlewood,<sup>3</sup> and Darryl L. Smith<sup>1</sup>

<sup>1</sup>*Theoretical Division, Los Alamos National Laboratory, Los Alamos, NM 87545*

<sup>2</sup>*National High Magnetic Field Laboratory, Los Alamos National Laboratory, Los Alamos, NM 87545*

<sup>3</sup>*Cavendish Laboratory, Madingley Road, Cambridge CB3 0HE, United Kingdom*

Ultracold alkali atoms [1, 2, 3, 4] provide experimentally accessible model systems for probing quantum states that manifest themselves at the macroscopic scale. Recent experimental realizations of superfluidity in dilute gases of ultracold fermionic (half-integer spin) atoms [5, 6, 7] offer exciting opportunities to directly test theoretical models of related many-body fermion systems that are inaccessible to experimental manipulation, such as neutron stars [8] and quark-gluon plasmas [9]. However, the microscopic interactions between fermions are potentially quite complex, and experiments in ultracold gases to date cannot clearly distinguish between the qualitatively different microscopic models that have been proposed [10, 11, 12, 13]. Here, we theoretically demonstrate that optical measurements of electron spin noise [14, 15] – the intrinsic, random fluctuations of spin – can probe the entangled quantum states of ultracold fermionic atomic gases and unambiguously reveal the detailed nature of the interatomic interactions. We show that different models predict different sets of resonances in the noise spectrum, and once the correct effective interatomic interaction model is identified, the line-shapes of the spin noise can be used to constrain this model. Further, experimental measurements of spin noise in classical (Boltzmann) alkali vapors are used to estimate the expected signal magnitudes for spin noise measurements in ultracold atom systems and to show that these measurements are feasible.

PACS numbers: 03.75.Hh, 03.75.Ss, 05.30.Fk

Owing to their perceived simplicity, the properties of dilute degenerate fermionic systems are sometimes attributed universal character [16], an assertion that must be called into question if the interaction between degenerate alkali atoms turns out to be complex. It is thus unfortunate that the nature of the effective interatomic interactions remains an outstanding fundamental issue. Specifically, the role played by the underlying hyperfine atomic-level structure is not yet understood. To date, experiments on ultracold fermionic atom gases can be interpreted equally well using qualitatively different models for the effective interactions, such as the Fermi-Bose [10, 11] or the multi-level models [12, 13]. Hence, new experimental observables are needed to distinguish between these competing models, and the principal distinctions between current models will lie in their predicted excitation spectra, which are not yet well studied.

The excitation spectra of physical systems are often studied by measuring their response to an external perturbation. Alternatively, measuring the spectrum of intrinsic fluctuations of a physical system can provide the same information, and these “noise spectroscopies” often disturb the physical system less strongly and scale more favorably with system size reduction. At very low temperature, noise from quantum fluctuations of an observable that does not commute with the Hamiltonian of the system can be used as a probe of the system properties. Electron spin is not a good quantum number in alkali gases, and fluctuations of electron spin can be measured using optical Faraday rotation. The electron spin noise spectrum consists of a series of resonances occurring at

frequencies corresponding to the difference between hyperfine/Zeeaman atomic levels. The integrated strength of the lines gives information about the occupation of the atomic levels, while the line shapes depend on the properties of the condensed atomic state. It is precisely the spectroscopic nature of the electron spin noise measurement that allows it to distinguish between various many-body models for the quantum states of ultracold fermionic atom gases: different models predict entirely different sets of resonances in the noise spectrum, and once the correct effective interatomic interaction model is identified, the line-shapes of the spin noise can be used to constrain this model.

To measure the electron spin noise via Faraday spectroscopy, a linearly polarized laser beam, with photon energy tuned near but not exactly on the s-p optical transition of the outer s-orbital electron, traverses an ensemble of alkali atoms [14]. The rotation angle of the laser polarization traversing the sample is measured as a function of time. The time average of this rotation angle vanishes, but the noise power spectrum of the rotation angle shows distinct peaks. In the electronic ground state (s-orbital) there is a strong hyperfine coupling between the nuclear and electron spins. For the electronic p-orbital, the hyperfine splitting is weak, however there is a strong spin-orbit coupling between the p-orbital and its spin. The laser photons directly couple to the spatial part of the electron wave function, but because of the spin-orbit splitting in the final state of the optical transition there is an indirect coupling between the laser photons and the electron spin. A fluctuating birefringence, that is a dif-

ference in refractive index for left and right hand circular polarizations, results from quantum fluctuations in the electron spin and leads to rotation of the polarization angle of the laser. The experiment is sensitive to fluctuations of electron spin projection in the direction of laser propagation.

The Hamiltonian describing the system of alkali atoms consists of a sum of one- and two-atom terms. The one-atom Hamiltonian includes the kinetic energy, the Zeeman interaction, and the hyperfine interaction between the nuclear spin  $\vec{I}$  and the electron spin  $\vec{s}$ . The single-atom eigenvectors, the starting point for describing the many-body system, are obtained by diagonalizing the one-atom Hamiltonian. This Hamiltonian preserves the projection of total angular momentum,  $\vec{F} = \vec{s} + \vec{I}$ , in the direction of the applied magnetic field. The one-atom matrix elements can be grouped into 2-dimensional blocks involving the basis states  $|I m_I\rangle|\frac{1}{2}\frac{1}{2}\rangle$  and  $|I m_I + 1\rangle|\frac{1}{2} - \frac{1}{2}\rangle$ , except for the states  $|I, m_I = +I\rangle|\frac{1}{2}\frac{1}{2}\rangle$ , and  $|I, m_I = -I\rangle|\frac{1}{2} - \frac{1}{2}\rangle$ , which do not couple. The single-atom energies vary smoothly and do not cross with increasing magnetic field so the single-atom states can be labelled unambiguously by,  $|F m_F\rangle$ , where  $m_F$  is a good quantum number, but  $F$  is only a good quantum number at zero magnetic field.

In general, the projections of electron spin are not good quantum numbers of the one atom Hamiltonian. At magnetic fields where the hyperfine interaction is comparable or larger than the Zeeman splitting, the electron and nuclear spins are entangled and no projection of electron spin is a good quantum number. At strong magnetic fields, where the Zeeman splitting is much larger than the hyperfine interaction, the electron spin projection in the direction of the magnetic field becomes a good quantum number, but electron spin projection orthogonal to the magnetic field is not. Faraday rotation is sensitive to fluctuations of the electron spin in the laser propagation direction. Thus at magnetic fields where the hyperfine interaction is comparable or larger than the Zeeman splitting, noise spectroscopy can be performed with the magnetic field either parallel or orthogonal to the direction of laser propagation whereas in the opposite limit, the magnetic field must be orthogonal to the direction of laser propagation.

For a Gaussian optical beam profile, the polarization rotation angle noise is

$$\frac{\phi_N(\omega)}{\sqrt{\delta f}} = C \left[ \frac{\sqrt{\pi}}{2} \frac{L \rho_0}{A} S(\omega) \right]^{1/2}, \quad (1)$$

where

$$C = \frac{2\pi}{3} \frac{c r_0}{m_0} \frac{1}{\hbar \Omega} \frac{|\langle S|p_x|P_x\rangle|^2}{|\Omega_{s-p} - \Omega|}. \quad (2)$$

Here  $\rho_0$  is the density of atoms,  $\Omega$  is the angular frequency of the laser,  $\Omega_{s-p}$  is the angular frequency of the

optical resonance,  $r_0$  is the classical electron radius,  $m_0$  is the electron mass,  $\langle S|p_x|P_x\rangle$  is the momentum matrix element for the optical transition, and the optical beam area is  $A = \pi q_0^2$  where  $q_0$  is the radius at which the beam intensity drops to  $1/e$  of its peak value. The electron spin response function  $S(\omega)$  is

$$S(\omega) = \frac{1}{\rho_0} \int dt e^{i\omega t} \int d^3r \langle \sigma_z(\mathbf{r}, t) \sigma_z(0, 0) \rangle, \quad (3)$$

where  $z$  is the direction of laser propagation,  $\sigma_z(\mathbf{r}, t)$  is twice the  $z$ -projection of the electron spin density operator, and  $S(\omega)$  satisfies the sum rule

$$\int d\omega S(\omega) = 2\pi. \quad (4)$$

The spin response function  $S(\omega)$  has peaks at frequencies near the separation between single atom spin levels

$$S(\omega) = \sum_{ij} |\langle i|\sigma_z|j\rangle|^2 S^{i \rightarrow j}(\omega), \quad (5)$$

where  $\{i, j\}$  label the single atom spin levels  $|\langle i|\sigma_z|j\rangle|^2$  is a one atom matrix element that determines line strengths and selection rules, and  $S^{i \rightarrow j}(\omega)$  contains information about the many-body state. The response function

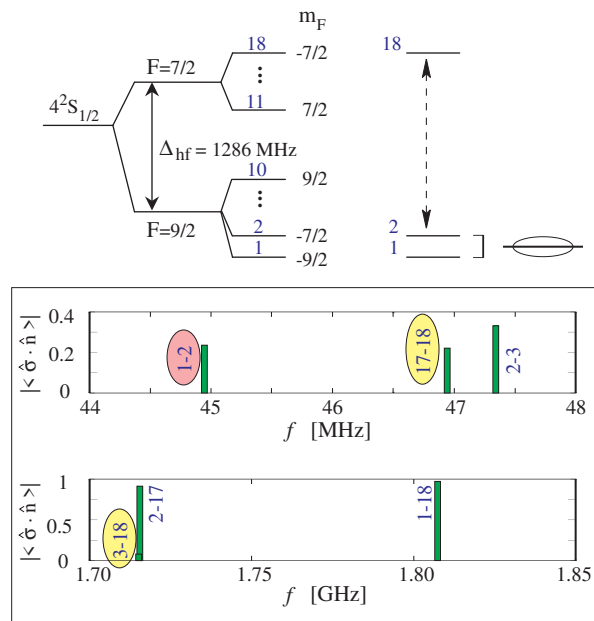


FIG. 1: [top] The Zeeman structure of  $^{40}\text{K}$  ( $I=4$ ), together with schematics of the 3- and 2-level models. In the 2-level model, only the two lowest hyperfine states are present. [bottom] Expected spin noise spectrum at the Feshbach resonance ( $B = 202$  G), for laser propagation orthogonal to the magnetic field. The highlighted transitions are not present in the 2-level model, but are predicted in the 3-level model [12]. In the 2-level model, lines 17 – 18 and 3 – 18 are forbidden, and line 1 – 2 has zero strength. Lines 3 – 18 and 2 – 17 are almost degenerate.

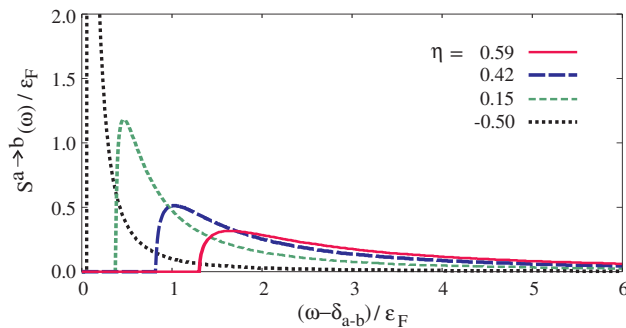


FIG. 2: Line-shapes for Type B transitions in the 2-level model. Type A transitions have zero strength in the 2-level model.

$S^{i \rightarrow j}(\omega)$  will only have strength if at least one of the states  $i$  or  $j$  has nonzero occupation. For laser propagation orthogonal to the magnetic field the selection rules require that the one-atom quantum number,  $m_F$  change by  $\pm 1$  between the two single atom levels.

Equations (1) and (2) show that the noise signal decreases linearly with inverse frequency detuning from the optical resonance. By contrast, the energy dissipated into the atomic system, either by optical absorption or Raman scattering, decreases quadratically with inverse frequency detuning. Thus noise spectroscopy measurements are weakly perturbative in the sense that the noise spectroscopy signal decreases more slowly with inverse frequency detuning than does the energy dissipated into the system.

The line shape of the response function  $S^{i \rightarrow j}(\omega)$  gives information about the many-body quantum state which depend on the interatomic interaction. In current experiments, the system is initially prepared by equally populating the two lowest hyperfine states. However, subsequent variation of the magnetic field, induces virtual scattering processes of particles between all *interacting* atomic states. Most of the available experimental data, can be successfully interpreted in the framework of the 2-level model [17, 18, 19, 20], which only includes interactions between the lowest hyperfine levels. Spin noise spectroscopy can access physics beyond the 2-level model, and distinguish between Fermi-Bose [10, 11] and multi-level Hamiltonian models [12, 13].

A gas of  $^{40}\text{K}$  atoms ( $I = 4$ ) is an especially promising system for studying models of the effective two-body interatomic interaction [12]. For  $^{40}\text{K}$  the subspace of interacting atomic states is very restrictive, because the hyperfine coupling constant is negative so that the lowest energy state is  $m_F = -\frac{9}{2}$ . Experimentally,  $^{40}\text{K}$  atoms are trapped in the two lowest hyperfine states,  $|\frac{9}{2}, -\frac{9}{2}\rangle$  and  $|\frac{9}{2}, -\frac{7}{2}\rangle$ . In the s-wave limit, the open channel can couple to only *one* closed-channel state  $|\frac{7}{2}, -\frac{7}{2}\rangle$ , and the interacting part of the Hamiltonian reduces to a 3-level system. Figure 1 shows the schematics of the  $^{40}\text{K}$  struc-

ture, and the 3-level Feshbach resonance model [12]. We denote the atomic states  $|\frac{9}{2}, -\frac{9}{2}\rangle$ ,  $|\frac{9}{2}, -\frac{7}{2}\rangle$ , and  $|\frac{7}{2}, -\frac{7}{2}\rangle$ , as 1, 2 and 18, respectively. In Fig. 1 we also plot the expectation values of the spin-projection operators for transitions in the 3-level model.

In the 2-level model, the noise spectrum consists of lines corresponding to occupied-to-occupied and occupied-to-unoccupied states transitions. We use the Hartree-Fock-Bogoliubov (HFB) formalism to calculate the zero temperature spin-spin response functions  $S^{i \rightarrow j}(\omega)$ . We find that the spin-spin response function corresponding to a transition between two occupied states is

$$S^{1 \rightarrow 2}(\omega) = \frac{1}{\rho_0} N(k_E) [(1 - \rho_{k_E}) \rho_{k_E} - \kappa_{k_E}^2]_{E=(\omega - \delta_{12})}, \quad (6)$$

where  $N(k)$  is the density of states, and  $\rho_k = \langle a_k^\dagger a_k \rangle$  and  $\kappa_k = \langle a_k a_k \rangle$  are the normal and anomalous densities, respectively. In Eq. (6) we denote by  $\delta_{12}$  the energy separation between levels 1 and 2. In the case of a transition from an occupied ( $a$ ) to an unoccupied state ( $b$ ), the corresponding spin-spin response function becomes

$$S^{a \rightarrow b}(\omega) = \frac{1}{\rho_0} [N(k_E) \rho_{k_E}]_{E_k + (\epsilon_k - \mu) = \omega - \delta_{ab}}, \quad (7)$$

where  $\mu$  is the chemical potential such that  $N_1 = N_2 = \rho_0/2$ . Since, for any  $k$  value,  $\rho_k^2 + \kappa_k^2 = \rho_k$ , the strength

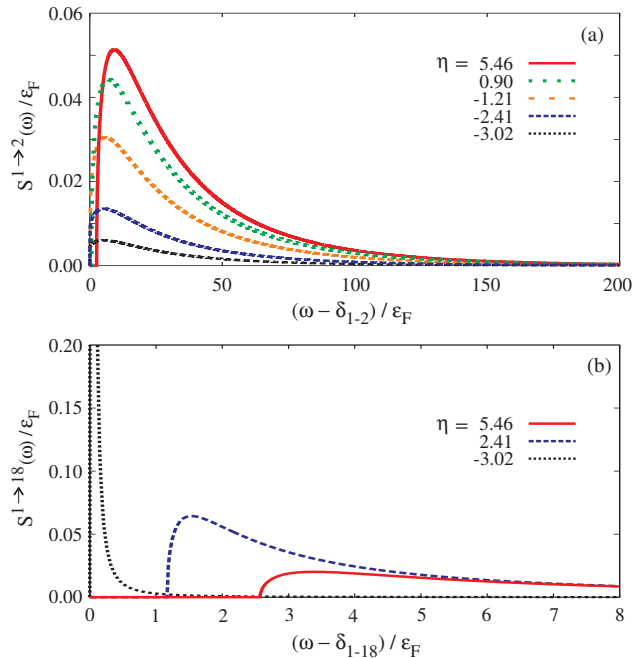


FIG. 3: Line-shapes in the 3-level model for  $^{40}\text{K}$ .  $S^{1 \rightarrow 2}$  and  $S^{1 \rightarrow 18}$  are examples of Type A and Type B transitions, respectively. In the non-interacting limit, the lines of Type B become  $\delta$ -functions while the lines of Type A disappear.

of the  $1 \rightarrow 2$  (occupied-to-occupied, or Type A) transition vanishes in the 2-level model. The 2-level model for the line shape of the occupied-to-unoccupied (Type B) transitions depends on the dimensionless parameter  $\eta = (k_F a)^{-1}$  (see Fig. 2). Here  $k_F$  is the Fermi momentum, and  $a$  is the s-wave scattering length. In the normal phase ( $a \rightarrow -0$ ), the line shape of a Type B transition becomes a delta-function located at the energy separation between levels 1 and 2. On the BCS side, the quasi-particle dispersion exhibits a local minimum at a finite momentum value, and the corresponding singularity in the density of states [20], is reflected by the characteristic shape of the spin-spin correlation function. On the BEC side of the crossover, the singularity in the density of states is located at zero momentum, and the spin-spin correlation function has a smooth shape. The line shape of a Type B transition in the 2-level model provides an unambiguous signature for the presence of fermionic superfluidity in the system.

The 3-level model involves the lowest two hyperfine levels, 1 and 2, plus the topmost hyperfine state denoted by 18. In this model, the particle number constraint becomes  $N_1 = N_2 + N_{18} = \rho_0/2$ . Figure 3 shows the characteristic shape of the lines predicted by the 3-level model, as a function of the dimensionless parameter  $\eta = (k_F a)^{-1}$ . The top panel illustrates the line shape of Type A transitions, such as  $1 \rightarrow 2$ . The line shapes for Type B transitions are shown in the bottom panel. The contrast between the predictions of the 2-level and the 3-level model are evident: In the 2-level model, the tran-

sitions between the occupied levels,  $1 \rightarrow 2$ , have zero strength independent of  $\eta$ , while in the 3-level model the strength of the  $1 \rightarrow 2$  transitions is *nonzero*. The transitions  $17 \rightarrow 18$ , and  $3 \rightarrow 18$  are allowed in the 3-level model, but not in the 2-level model.

Because of the sum rule (4), the expected signal strength for spin noise measurements in ultracold atom gases can be estimated from corresponding measurements in classical alkali gases. The theoretical results of Eq. (1) apply to both classical and quantum gases. The parameters in Eq. (1) are the same for the various isotopes of a given alkali atom. Figure 4 shows measured spectra of spin noise in a vapor of  $^{41}\text{K}$  atoms at 184 °C. The discrete peaks, readily visible above the white noise floor, result from electron spin fluctuations. The integrated spin noise of the four peaks are 1.3, 2.3, 2.6, and 2.1  $\mu\text{rad}$ , respectively. The ratios of the measured integrated spin noise powers compare very well with the theoretical results from Eq. (1). The overall magnitude of the detected spin noise is a factor 2.7 lower than theoretical expectation, which may result from uncertainties in the laser beam diameter. In an ultracold gas of potassium atoms with a density of  $10^{13} \text{ cm}^{-3}$  and a trap length of 0.2 mm, we expect a similar magnitude for the noise peaks with a 20 micron diameter laser detuned 15 GHz from the optical resonance. In ultracold fermionic atom gases the frequency detuning can be significantly less than 15 GHz and thus much larger noise signals than shown in Fig. (4) should be achievable. We conclude that spin noise measurements in ultracold gases of alkali atoms are feasible.

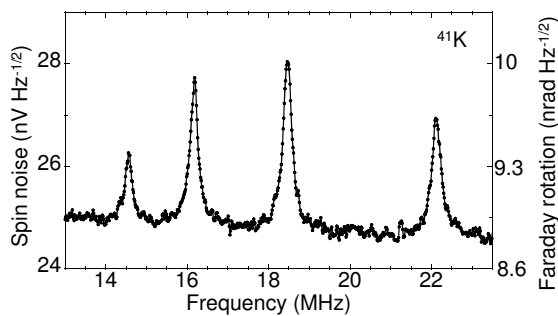


FIG. 4: Spectra of spin noise, measured via Faraday rotation, in a  $^{41}\text{K}$  vapor at 184 °C (density  $N = 7.3 \times 10^{13} \text{ cm}^{-3}$ ). Peaks correspond to  $\Delta m_F = \pm 1$  transitions. The probe laser (4 mW) is detuned 100 GHz from the D1 transition ( $4S_{1/2} - 4P_{1/2}$ ; 770 nm), and  $B_{\perp} = 25.6 \text{ G}$ . The vapor is contained in a 10 mm long cell, and the laser beam diameter (to 1/e peak intensity) is 65  $\mu\text{m}$ . The noise data are shown in units of voltage ( $\text{nV Hz}^{-1/2}$ ), and Faraday rotation fluctuations ( $\text{nrad Hz}^{-1/2}$ ). The white noise floor is primarily from photon shot noise and amplifier noise. The discrete peaks show noise from electron spin fluctuations and have integrated values of 1.3, 2.3, 2.6, and 2.1  $\mu\text{rad}$ . Similar signal magnitudes are expected in ultracold atom systems (see text).

In summary, we have shown that electron spin noise spectroscopy can be used to probe the quantum states of ultracold fermionic atomic gases. The measurements proposed here have the unique ability to unambiguously reveal the nature of the effective interactions present in these systems, and to distinguish between various many-body models for the quantum states of these systems. As a consequence, the 2-level model predicts that transitions between occupied atomic levels will have zero strength [21]. In contrast multi-level Hamiltonians allow for such transitions. In particular, ultracold  $^{40}\text{K}$  atom gases represent an ideal test case, because the mechanism of the s-wave Feshbach resonance in this system consists of only three interacting atomic levels.

**Acknowledgments** This work was supported in part by the LDRD program at Los Alamos National Laboratory. B.M. acknowledges financial support in covering part of his travel expenses to Cambridge through the ICAM fellowship program. We thank M.M. Parish and A.V. Balatsky for valuable discussions.

Correspondence and requests for materials should be addressed to B.M. (bmihaila@lanl.gov).

- 
- [1] Anderson, M.H. Ensher, J.R., Matthews, M.R., Wieman, C.E., & Cornell, E.A., Observation of Bose-Einstein condensation in a dilute atomic vapor, *Science* **269**, 198 (1995).
- [2] Davis, K.B. *et al.*, Bose-Einstein condensation in a gas of sodium atoms, *Phys. Rev. Lett.* **75**, 3969 (1995).
- [3] Bradley, C.C., Sackett, C.A., Tollet, J.J., & Hulet, R.G., Evidence of Bose-Einstein condensation in an atomic gas with attractive interactions, *Phys. Rev. Lett.* **75**, 1687 (1995).
- [4] DeMarco, B. & Jin, D.S., Onset of Fermi Degeneracy in a Trapped Atomic Gas, *Science* **285**, 1703 (1999).
- [5] Regal, C.A., Greiner, M. & D.S. Jin, Observation of resonance condensation of fermionic atom pairs, *Phys. Rev. Lett.* **92**, 040403 (2004).
- [6] Bartenstein, M. *et al.*, Collective excitations of a degenerate gas at the BEC-BCS crossover, *Phys. Rev. Lett.* **92**, 203201 (2004).
- [7] Zwierlein, M.W. *et al.*, Condensation of pairs of fermionic atoms near a Feshbach resonance, *Phys. Rev. Lett.* **92**, 120403 (2004).
- [8] Yakovlev, D.G. and Pethick, C.J., Neutron star cooling, *Annu. Rev. Astrophys.* **42**, 169 (2004).
- [9] Meyer-Ortmanns, H., Phase transitions in quantum chromodynamics, *Rev. Mod. Phys.* **68**, 473 (1996).
- [10] Holland, M., Kokkelmans, S.J.J.M.F., Chiofalo, M.L., & Walser, R., *Phys. Rev. Lett.* **87**, 120406 (2001).
- [11] Timmermans, E., Furuya, K., Milonni, P.W., & Kerman, A.K., Prospect of creating a composite Fermi-Bose superfluid, *Phys. Lett. A* **285**, 228 (2001).
- [12] Parish, M.M., Mihaila, B., Simons, B.D., & Littlewood, P.B., Fermion-mediated BCS-BEC crossover in ultracold K-40 gases, *Phys. Rev. Lett.* **94**, 240402 (2005).
- [13] Bruun, G.M., Jackson, A.D. & Kolomeitsev, E.E., Multichannel scattering and Feshbach resonances: Effective theory, phenomenology, and many-body effects, *Phys. Rev. A* **71**, 052713 (2005).
- [14] Crooker, S.A., Rickel, D.G., Balatsky, A.V., & Smith, D.L., Spectroscopy of spontaneous spin noise as a probe of spin dynamics and magnetic resonance, *Nature* **431**, 49 (2004).
- [15] Oesterich, M., Römer, M., Haug, R.J., & Hägele, D., Spin noise spectroscopy in GaAs, *Phys. Rev. Lett.* **95**, 216603 (2005).
- [16] Heiselberg, H., Fermi systems with long scattering lengths, *Phys. Rev. A* **63**, 043606 (2001).
- [17] Leggett, A.J., Diatomic molecules and Cooper pairs, in *Modern Trends in the Theory of Condensed Matter*, edited by A. Pekalski & R. Przystawa (Springer-Verlag, Berlin, 1980).
- [18] Comte, C. & Nozières, P., Exciton Bose condensation: the ground state of an electron-hole gas I. Mean field description of a simplified model, *J. Phys.* **43**, 1069 (1982).
- [19] Nozières, P. & Schmitt-Rink, S., Bose condensation in an attractive fermion gas: from weak to strong coupling superconductivity, *J. Low Temp. Phys.* **59**, 195 (1985).
- [20] Parish, M.M., Mihaila, B., Timmermans, E.M., Blagoev, K.B. & Littlewood, P.B., BCS-BEC crossover with a finite-range interaction, *Phys. Rev. B* **71**, 064513 (2005).
- [21] B. Mihaila *et al.*, Density and spin response functions in ultracold fermionic atom gases, *Phys. Rev. Lett.* **95**, 090402 (2005).